

# Pool Boiling Heat transfer over micro-treated surfaces: a Mechanistic Approach

Emanuele Teodori<sup>1, a</sup>, Ana S. Moita<sup>1, b</sup> and António L. N. Moreira<sup>1, c</sup>

<sup>1</sup>IN+ - Center for Innovation, Technology and Policy Research, Instituto Superior Técnico, University of Lisbon. Av. Rovisco Pais 1, 1049-001 Lisbon, Portugal.

[e.teodori@dem.ist.utl.pt](mailto:e.teodori@dem.ist.utl.pt), [anamoita@dem.ist.utl.pt](mailto:anamoita@dem.ist.utl.pt), [moreira@dem.ist.utl.pt](mailto:moreira@dem.ist.utl.pt)

**Keywords:** Pool boiling heat transfer, micro-treated surfaces, mechanistic approach, bubble dynamics, interaction mechanisms.

**Abstract.** This paper introduces a quantitative description of the most relevant parameters characterizing bubble dynamics on pool boiling over micro-treated surfaces. From the revised theoretical descriptions, analyzed against the experimental data, the importance of quantifying the interaction mechanisms is evidenced. Such importance was shown at the bubble departure diameter and at the nucleation sites density. Based on this analysis, some corrections are proposed. At the end, the most relevant parcels of the heat flux are determined following a mechanistic approach, with satisfactory results. This is the first step towards the presentation of a mechanistic approach to model the bubble dynamics and the heat transfer mechanisms over enhanced surfaces.

## Introduction

Several studies in the literature confirmed the potentiality of surface structuring in enhancing the pool boiling heat transfer [1]. The approach followed in the interpretation of the results is however often empiric, leading to non-universal conclusions on the role of interface modification on the heat transfer mechanisms. A mechanistic approach would be more suitable for a better understanding of the phenomena occurring during the boiling process and particularly when surface modification and bubble interaction are involved. Few of these mechanistic approaches have been followed in the past to predict basic bubble dynamics parameters (e.g. bubble departure diameter [2], departure frequency [3]), which are then used to evaluate the heat transfer, as recently proposed in the experimental work of Gerardi *et al.* [4] and in numerical studies of Son and Dhir [5] and of Hazi and Markus [6]. Nonetheless, the available theoretical relations do not agree with the experimental data particularly when extreme wetting conditions occur (e.g. [7]). Also, very few data and theoretical studies are available to describe the effect of bubble interaction mechanisms. In this context, a big effort is required to gather data related not only to the heat transfer, but also to the bubble dynamic and to the evaluation of the effect of bubble interaction for different liquid/surface combination.

In line with this, the present paper introduces the first approach to a mechanistic model, which identifies the main parameters to include in the model, that are affected by the liquid properties, surface topography and the induced interaction among nucleation sites. The liquid properties are varied using a range of fluids, namely water, ethanol and a dielectric fluid HFE7000, which were selected to have a gradual variation in the properties that are most relevant for pool boiling heat transfer (e.g. density, surface tension, thermal conductivity, heat capacity and latent heat of evaporation). Then, after a critical analysis of these parameters, they are used to estimate the various parcels of the heat transfer and thus to discuss the influencing effects on these parcels. The obtained results are finally used to discuss some of the phenomena characterizing the pool boiling.

## Experimental Set-up and Measurement Procedures

Pool boiling is investigated for various liquids, namely the dielectric fluid HFE 7000, ethanol and water, whose relevant thermal properties are shown in Table 1. Heat flux and heat transfer coefficients are determined for the various pairs liquid/surface. Afterwards, they are related to the bubble dynamics. This characterization is made by combining high-speed visualization with PIV measurements. Complete description of the measurement procedures and corresponding uncertainties is detailed in Teodori *et al.* [8].

**Table 1** Thermophysical properties of the liquids used in the present study, taken at saturation, at  $1.013 \times 10^5 \text{ Pa}$ .

Property	Ethanol	Water	HFE7000
Saturation temp. - $T_{\text{sat}}$ [ $^{\circ}\text{C}$ ]	78.4	100	34
Liquid density - $\rho_l$ [ $\text{kg}/\text{m}^3$ ]	736.4	957.8	1374.7
Vapor density - $\rho_v$ [ $\text{kg}/\text{m}^3$ ]	1.647	0.5956	4.01
Liquid dynamic viscosity - $\mu_l$ [ $\text{mN m}/\text{s}^2$ ]	0.448	0.279	0.3437
Liquid specific heat - $c_{pl}$ [ $\text{J}/\text{kg}$ ]	3185	4217	1352.5
Liquid thermal conductivity - $k_l$ [ $\text{W}/\text{mK}$ ]	0.165	0.68	0.07
Latent heat of evaporation - $h_{lg}$ [ $\text{kJ}/\text{kg}$ ]	849.9	2257	142
Liquid surface tension - $\sigma_{lv}$ [ $\text{N}/\text{m}$ ] $\times 10^3$	17	58	12.4

The surfaces are micro-structured with custom regular patterns produced over silicon wafers by combining wet etching with plasma etching. Topographic profiles were measured with a Dektak 3 contact profilometer (Veeco) with a precision of  $\pm 100 \text{ \AA}$ . Wettability was also characterized, being quantified by the static contact angle  $\theta$ , using an optical tensiometer THETA from Attension, with One-Attension v1.8 software. Accuracy of the measures of the contact angle is  $\pm 1^{\circ}$ , according to the manufacturer. Table 2 depicts the main topographical characteristics of the surfaces used in this study. The table includes the average values of the static contact angles, which were measured as described in [9]. The contact angles obtained with ethanol and HFE7000 in contact with all the surfaces are close to zero. The patterns are composed by regular arrays of squared cavities, with fixed size length  $a=52 \text{ }\mu\text{m}$  and fixed depth  $h_R=20\mu\text{m}$ . The distance between the centers of the cavities,  $S$  is mainly our optimization variable, ranging between  $300\mu\text{m} < S < 1200\mu\text{m}$ .

**Table 2** Main range of the topographical characteristics of the micro-patterned surfaces.  $\theta$  is the average static contact angle measured with water at room temperature.  $\theta \cong 0^{\circ}$  for all the surfaces in contact with ethanol and HFE7000.

Material	Reference	$a$ [ $\mu\text{m}$ ]	$h_R$ [ $\mu\text{m}$ ]	$S$ [ $\mu\text{m}$ ]	$\theta$ [ $^{\circ}$ ]
Silicon	Smooth	$\approx 0$	$\approx 0$	$\approx 0$	86.0
Wafer	C1	52	20	304	90.0
	C2	52	20	400	91.5
	C3	52	20	464	71.5
	C4	52	20	626	86.5
	C5	52	20	700	95.0
	C6	52	20	800	60.5
	C7	52	20	1200	66.3

Most of the results presented here were obtained with the experimental arrangement described in [8]. However, a new set-up has been recently built, to allow more precise measurements and therefore validate those previously obtained. In particular a dynamic control of the pressure has been realized that would permit pressure variations lower than 5 mbar. More details of the new set-up will be explained in the future.

## Results and Discussion

Quantitative and qualitative analysis of the bubble dynamic and the nucleation mechanisms for the 3 chosen liquids, water, ethanol and HFE7000, allows deepening the understanding of the coupled effect of liquid properties and surface topography and to highlight the importance of considering a mechanistic approach. Differences between the boiling of the 3 fluids is evidenced in Fig. 1, which depicts the bubble departure diameter, departure frequency and nucleation sites density for the boiling of the 3 fluids over the micro-structured surfaces, as identified as in Table 2.

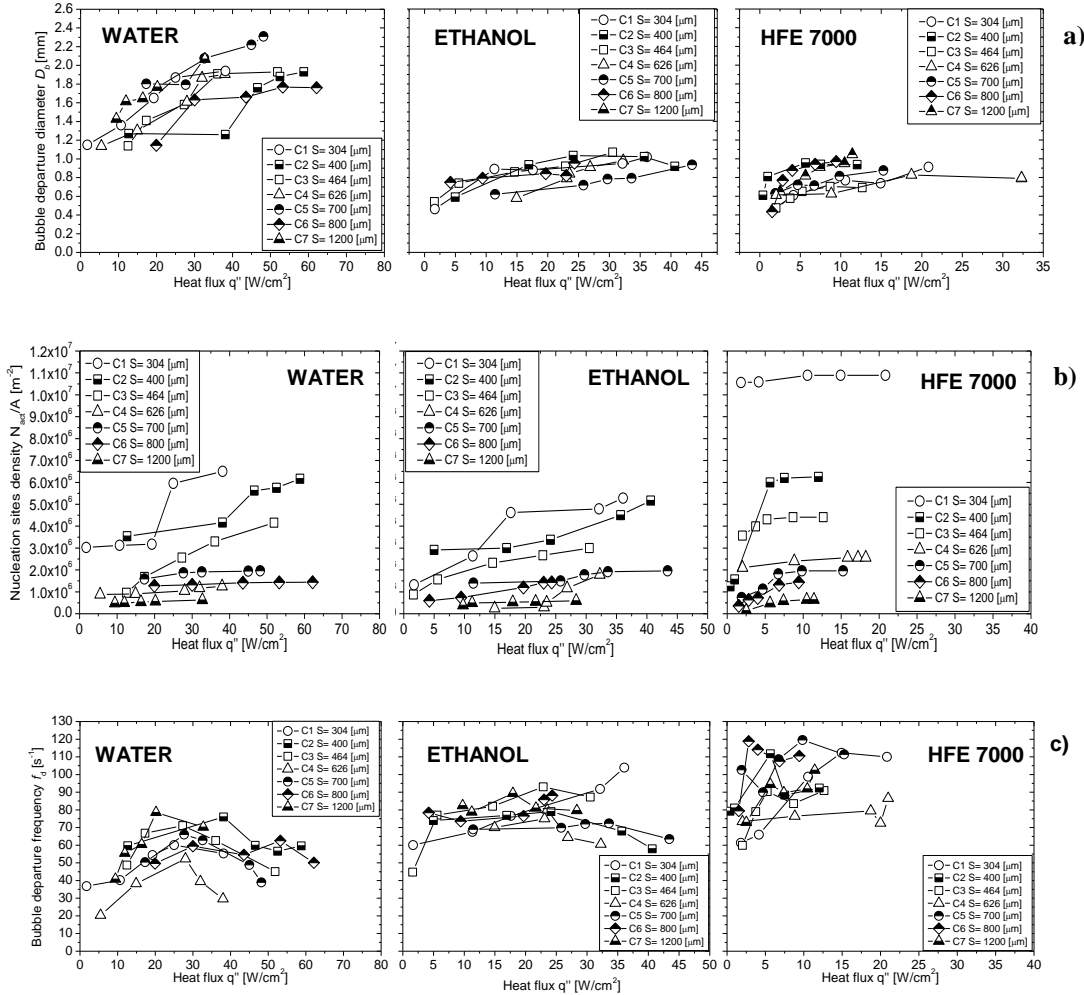


**Fig. 1.** Bubble dynamics in pool boiling of water, ethanol and HFE7000 over micro-structured surfaces: a) bubble departure diameter, b) nucleation sites density, c) bubble departure frequency.

Analyzing the results in Fig. 1 from a mechanistic approach, by simply considering that bubble departure depends on the balance between surface flux tension forces ( $\sim \sigma_{lv} D_b^2$ ) and the buoyancy forces ( $\sim g(\rho_l - \rho_v)$ ), the largest bubbles are expected in water boiling, which is confirmed in the figure. Here, we are for now neglecting additional effects of the shear lift and drag forces which may act to favour buoyancy effects, as discussed in [7]. Due to the lowest dimensions of the bubbles and to the more homogeneously distributed boiling process, HFE7000 was found to be the liquid with the highest value of nucleation sites on top of the structured surfaces (Fig 1b). Also, the boiling of this fluid resulted in the highest relative increase of the number of nucleation sites, when compared to the number of cavities etched in the surface, i.e. the relation number of active nucleation sites/number of cavities is the highest. The lowest relation is observed for the boiling of water. This is a non-intuitive result, since the highest value of surface tension of the water should promote more unwetted cavities, thus facilitating the formation of bubbles. Nevertheless one must keep in mind that the largest dimensions of the bubbles avoids simultaneous presence of all the active nucleation sites on top of the surface, thus the actual nucleation sites are lowered. These bubbles also stay at

sites on top of the surface, thus the actual nucleation sites are lowered. These bubbles also stay attached to the surface for longer periods of time, thus allowing stronger interaction mechanisms such as horizontal coalescence. As a result, the bubble departure frequency for the boiling of water is declined for higher values of the heat fluxes, where typically the interactions mechanisms are stronger (Fig 1c). The opposite effects are observed in the boiling of HFE7000, which depicts the highest bubble departure frequency. In previous work, (e.g. Moita *et al.* [9]) an optimization of the distance between cavities  $S$  was experimentally performed, which allowed identifying a minimum value of  $S$  around  $400\mu\text{m}$  for water boiling, below which the boiling process and, consequently the heat transfer were significantly deteriorated, due to the very strong interaction mechanisms. These results evidence the need to include parameters to quantify these interaction mechanisms. In [9], for experimental data obtained for water and ethanol, a new parameter was proposed to quantify the horizontal coalescence, the coalescence factor  $D_b/D$ , where  $D_b$  is the departure diameter including coalescence and  $D$  is the diameter without coalescence.  $D_b > 1$  reveals the presence of horizontal coalescence. The coalescence factor vs the heat flux was reported in [10] for these 3 liquids. Such results clearly highlight the highest values of the coalescence factor, obtained for water boiling, thus confirming the strong influence of horizontal coalescence for this fluid. Contrary, for ethanol and HFE 7000, the coalescence factor is always close to 1, which is associated to low horizontal coalescence phenomena.

In summary, from this analysis one may infer that water boiling is strongly affected by interaction phenomena that interfere with the enhancement of heat transfer obtained by structuring the surface, while ethanol and HFE 7000 are clearly less influenced by these phenomena. In practical terms this means that for water boiling, the distance between cavities  $S$  can only be reduced until a minimum level, while for the other fluids such distance can be further reduced, thus increasing the number of cavities and therefore of the number of active nucleation sites.

Regarding the theoretical description of the basic quantities used above to characterize bubble dynamics, one can find in the literature several relations to predict the bubble departure diameter, which are mostly derived from the force balance proposed by Fritz [2],  $\sigma_{lv}\pi D \sin \phi = (\rho_l - \rho_g) \cdot g \cdot \pi \cdot (2 + 3 \cos \phi - \cos^3 \phi) / 24 D^3$  where  $D$  is the diameter of the spherical bubble and  $\phi$  is the angle formed between the surface and the bubble interface. Various relations reported in the literature are plotted together with our experimental data in Fig. 2. Here,  $Ja$  is the Jakob number defined as  $(T_w - T_{sat}) \cdot c_{p,l} \cdot \rho_l / (\rho_l \cdot h_{lg})$ , following the nomenclature used in Table 2, for the liquid and vapor properties.  $T_w$  is the surface temperature. This relation stresses the importance of describing the phenomena occurring at the interface formed between the bubble and the surface. Only after this is performed, one can accurately describe the effect of the contact angle  $\phi$ , which has not yet been completely achieved (interesting approach was followed for instance in [5]). This is indirectly highlighted in the results of Matkovic and Koncar [7] that show how this kind of relations is very sensitive to variations in the values of  $\phi$ . On the other hand, Fig 3 shows a clear disagreement between the experimental data and the theoretical relations. This can be attributed to the fact that the interaction mechanisms are not included here. The effect of the interaction mechanisms is also very strong in the active nucleation sites. Son and Dhir [5] propose a relation to determine the actual number of active nucleation sites, based on the number of cavities  $N_{cav}$ ,  $N = (\pi N_{cav} / 4)^{1/2}$ . This approach is very practical, but, again, does not include the interaction mechanisms. For instance the horizontal coalescence will affect the effective nucleation sites density. In our case, the number of cavities is distributed in a square surface. Following a similar line of thought, but instead of simply considering the size of the bubbles, we weighed the  $N_{cav}$  by the inverse of the coalescence factor. The resulting theoretical value of the nucleation sites density  $N^*$  is plotted against the experimental values, in Fig. 3, taken from the data gathered in Fig 1, for different micro-structured surfaces and different values of the heat flux. Quantitatively, there is not yet an agreement, but  $N^*$  follows quite well the trend of the experimental data, particularly for the case of the water boiling at high heat fluxes, (Fig 3b) for which the nucleation sites density is

strongly affected by the horizontal coalescence. Hence the theoretical model must for certain account at least for the coalescence factor, which, from this empirical approach seems to be a representative parameter.

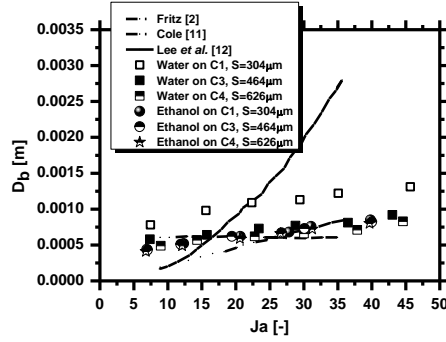


**Fig. 2.** Bubble diameter at departure, as a function of the Jakob number, for boiling over micro-structured surfaces: comparison between the experimental data and the correlations reported in the literature.

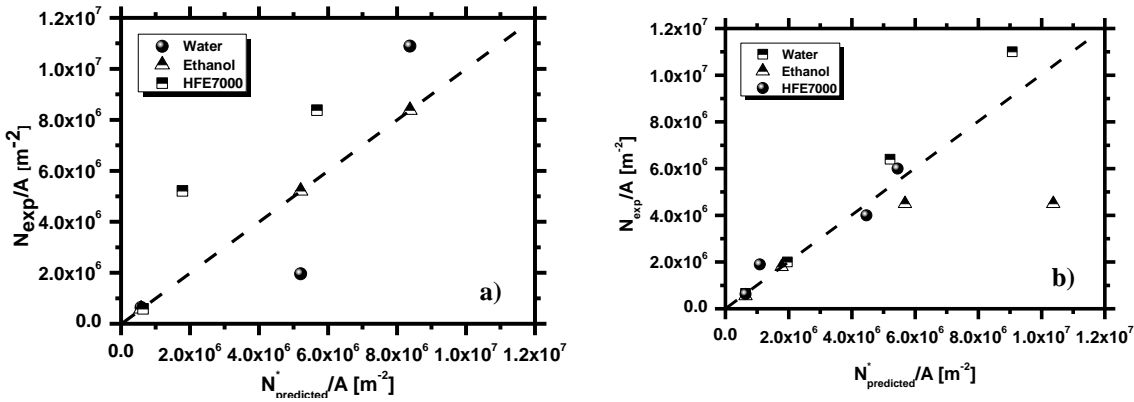


**Fig. 3.** Experimental vs predicted values of the active nucleation sites for the boiling of water, ethanol and HFE7000 at. a) Heat flux=10W/cm<sup>2</sup>, b) Heat flux=35W/cm<sup>2</sup>.

The aforementioned parameters, during bubble growing and detachment, will contribute with different weights to the final values of heat flux removed obtained. Based on this analysis, the heat flux was quantified, following the mechanistic approach considered for instance in [4]. Hence, 3 main parcels were evaluated, namely the natural convection

$$q''_{natconv} = \left[ 1 - \pi / 4A \sum_{n=1}^{N_T} (D_{b,n})^2 \right] h_{natconv} (T_w - T_{sat}), \text{ the latent heat parcel } q''_{ev} = \pi / 6A \rho_v h_{lg} \sum_{n=1}^{N_T} (f_n \cdot D_{3_{bn}})$$

and the enhanced convection  $q''_{ec} \propto f_b N_{ac} = q''_{tot} - q''_{natconv} - q''_{ev}$ . Here,  $A$  is the area of the heater,  $N_T$  is the total number of nucleation sites and  $N_{ac}$  is the number of active nucleation sites. From the results shown in Fig 4 a,b) it is worth noting that water does not present the highest relative values of heat removed by evaporation (Fig. 4a) despite being the fluid with the highest latent heat of evaporation. This is strongly related with the bubble nucleation. In fact, water pool boiling rendered lower values of nucleation sites in the surface, so that overall this parcel can be so low in comparison with the other fluids due to the lower number of nucleation sites removing heat from the surface. Clearly the plot shows that decreasing the number of cavities on the surface (thus increasing  $S$ ) bubble nucleation phenomena are attenuated decreasing the relative parcel of evaporation for the fluids that have a more vigorous boiling over surfaces with more cavities. So, in this case the latent heat of evaporation becomes important so water boiling presents, as expected, the highest relative heat removed by evaporation. Also the highest ebullition frequency of the fluid with lower surface tension can contribute to this kind of results. Fig. 4b) reports the relative parcel of heat removed by enhanced convection for the three fluids on structured surfaces. As expected, this parcel is the dominant, reaching values of almost the 90% for all the surfaces and all the fluids studied. Only water presented a relative decline of this value for the surface with sparser cavities, but this is

mostly related to the fact that, in this case, the parcel of heat removed by evaporation balanced the one removed by enhanced convection.

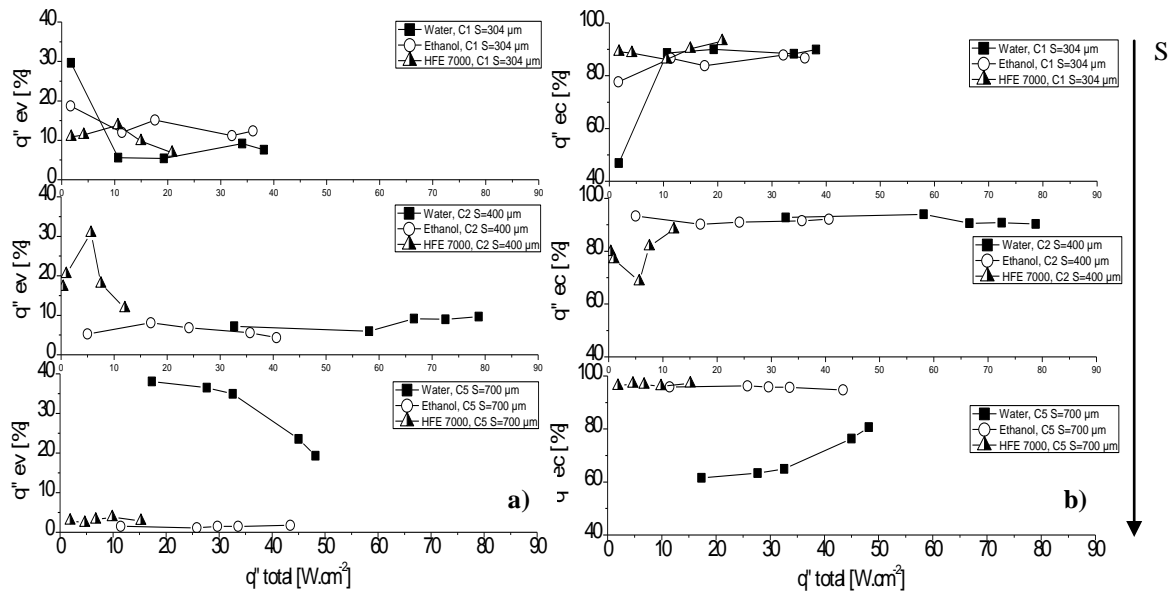


**Fig. 4.** Parcel of latent heat (left) and enhanced convection (right) for water, ethanol and HFE7000 on micro-structured surfaces (the distance between cavities,  $S$ , is increasing from top to the bottom).

## Final remarks

This paper introduces a quantitative description of the most relevant parameters characterizing bubble dynamics on pool boiling over micro-treated surfaces. The correct identification and description of these parameters is vital to obtain an accurate mechanistic model of the observed phenomena. From the revised theoretical descriptions, analyzed against the experimental data, the importance of quantifying the interaction mechanisms is evidenced. Such importance was shown at the bubble departure dynamics and at the nucleation sites density. Based on this analysis some corrections are proposed. At the end, the most relevant parcels of the heat flux are determined following a mechanistic approach with satisfactory results.

## Acknowledgments

The authors are grateful to Fundação para a Ciência e a Tecnologia (FCT) for partially financing the research under the framework of project PTDC/EME-MFE/109933/2009 and to support E. Teodori with a PhD Fellowship (Ref.:SFRH/BD/88102/2012). A.S. Moita also acknowledges the contribution of FCT for Post-Doc Fellowship (Ref.:SFRH/BPD/63788/2009).

## References

- [1] H. S. Ahn, H. J. Jo, H. Kang, M. H. Kim: Appl. Phys. Lett. Vol. 98(2011), p. 071908.
- [2] W. Fritz.: Physikalische Zeitschrift Vol.35 (1935), p. 379-388.
- [3] N. Zuber: Int. J. Heat Mass Transf. Vol 6 (1963), p. 53.
- [4] C. Gerardi, J. Buongiorno, L. Hu, T. McKrell: Int. J. Heat Mass Transf. Vol. 53 (2010), p. 4185.
- [5] G. Son, V. K. Dhir: Int. J. Heat Mass Transf. Vol. 51 (2008), p. 2566.
- [6] G. Hazi, A. Markus: Int. J. Heat Mass Transf. Vol. 52 (2009), p. 1472.
- [7] M. Matkocvic, B. Koncar: Science and Technology Nuclear Installations Vol. 2012: ID 863190, 7p.
- [8] E. Teodori, A. S. Moita, A. L. N. Moreira: Int. J. Heat Mass Transf. Vol. 66 (2013), p. 261.
- [9] A. S. Moita, E. Teodori, A. L. N. Moreira: Journal of Physics: Conf. Series 395: 012175 (2012).
- [10] E. Teodori, A. S. Moita, A. L. N. Moreira: Proceedings of ExHFT Lisbon (2013).
- [11] R. Cole: Chem. Eng. Progress Symp. Ser. Vol. 65 (1967), p. 211.
- [12] H. C. Lee, D. Oh, S. W. Bae, M. H. Kim: Int. J. Multiphase Flow Vol. 29 (2003), p. 1857.